J Biochem Technol (2026) 17(2): 60-70
https://doi.org/10.51847/g8pT52L1nd
ISSN: 0974-2328

Comparative Anti-Leishmanial Effects of Two ssDNA Aptamers Targeting Poly(A)-Binding Protein in *Leishmania donovani* Amastigotes

Haimn Abdulbassit Tawfiq*, Ahmed Ali Mohammed, Yassir Mustafa Kamal Al Mulla Hummadi

Received: 20 January 2026 / Received in revised form: 10 April 2026, Accepted: 15 April 2026, Published online: 25 May 2026

Abstract

Visceral leishmaniasis caused by *Leishmania donovani* is still a life-threatening disease with limited therapeutic options. The poly(A)-binding protein (PABP) is essential for post-transcriptional gene regulation in trypanosomatids and represents a parasite-privileged drug target. To comparatively evaluate two mechanistically distinct PABP-targeting ssDNA aptamers, AP-11 (poly(A)-competitive) and AP-7 (non-competitive), complexed with Lipofectamine 2000 against *L. donovani* amastigotes. Growth inhibition was assessed by MTT assay in amastigotes at 24 and 48 hours. Cytotoxicity was determined for selectivity index calculation in the RAW 264.7 cell line (Macrophage). PABP expression was demonstrated by western blot in both axenic culture and intracellular amastigote models. AP-11/LF demonstrated 4-6-times greater potency than AP-7/LF (IC_{50}: 130/80 nM versus 550/460 nM at 24/48 h). Both complexes exhibited favorable selectivity indices (47-84). AP-11/LF depleted PABP by >93% in axenic culture and about 80% in intracellular amastigotes ($p < 0.01$), whereas AP-7/LF produced moderate, inconsistently significant reductions (45-50%). Functional disruption of the PABP–poly(A) interaction, rather than binding affinity alone, determines antiparasitic potency, validating PABP as a pharmacologically tractable antileishmanial target. Remarkably, this is the first *in vitro* experimental study to demonstrate that aptamers targeting the PABP complexed with lipofectamine 2000 exert direct anti-leishmanial activity at both the axenic culture and intracellular levels.

Keywords: Poly(A)-binding protein, ssDNA aptamers, Visceral leishmaniasis, Intracellular amastigotes, RAW 264.7 Macrophages

Haimn Abdulbassit Tawfiq*
Department of Pharmacology and Toxicology, College of Pharmacy, Mustansiriyah University, Baghdad, Iraq.
Department of Pharmacology and Toxicology, College of Pharmacy, Ninevah University, Mosul, Iraq.

Ahmed Ali Mohammed
Department of Clinical Laboratory Sciences, College of Pharmacy, Mustansiriyah University, Baghdad, Iraq.

Yassir Mustafa Kamal Al Mulla Hummadi
Department of Pharmacology and Toxicology, College of Pharmacy, Mustansiriyah University, Baghdad, Iraq.

***E-mail:** haimn.abdulbassit@uoninevah.edu.iq

Introduction

Visceral leishmaniasis (VL), officially well-known as kala-azar, is one of the most lethal parasitic infections with an enormous effect on human well-being (Al Nasser *et al*., 2024; Zhang *et al*., 2025). Bone marrow, spleen, and liver are the most commonly infected organs having parasitized mononuclear phagocyte system (MPS), with hallmark symptoms of persistent fever, weight reduction, pancytopenia, and hepatosplenomegaly (Wamai *et al*., 2020; Kumar *et al*., 2022). The World Health Organization (WHO) addressed VL as one of the Neglected Tropical Diseases (NTD) in 2015 due to poor social awareness and continuous shortage of research funding for its therapies. WHO has reported that approximately 700,000 to 1,000,000 new cases of leishmaniasis occur each year, with more than 350 million individuals at risk of infection (Berry & Berrang-Ford, 2016; Knight *et al*., 2023; Huata-Panca *et al*., 2025). It carries a case-fatality rate of more than 95% when medical management is delayed, rendering it one of the most fatal parasitic diseases (Uliana *et al*., 2018). The current pharmacological management relies on a small number of chemotherapeutic reagents, with significant serious clinical limitations for each one. This treatment dilemma underscores the urgent need for new medications to avoid the well-known resistance while maintaining an acceptable safety profile (Pokharel *et al*., 2021; Pacheco-Fernandez *et al*., 2023; Alqara *et al*., 2024).

Trypanosomatid protozoans, such as leishmania, are characterized at the molecular level by their dependence on post-transcriptional regulatory mechanisms in controlling genetic expression. This is because conventional transcriptional regulation is absent, with the PABP playing a central role in this regulatory framework (Martínez-Calvillo *et al*., 2010; De Gaudenzi *et al*., 2011; Thuy *et al*., 2023). In leishmania, three different PABP homologues have been characterized. PABP1 is the primary cytoplasmic isoform that mediates cap-dependent translation through its preferential association with the eIF4E4/eIF4G3 initiation complex (Zinoviev & Shapira, 2012; Assis *et al*., 2021; Pham, 2024). Guerra *et al*. (2011) have cloned and functionally characterized the first PABP homologue from *L. infantum* (LiPABP), showing that this 65 kDa protein retains conserved RNA recognition motifs while harboring species-specific sequence divergences that differentiate it from mammalian analogs, positioning it as a possible diagnostic marker and therapeutic target (Guerra *et al*., 2011; Berzal-Herranz & Romero-López, 2024). According to the comparative sequence

analyses, PABP in Leishmania exhibits only 30-40% amino acid identity with the human counterpart. This level of structural variation could represent an adequate molecular base for parasite-selective pharmacological targeting (Bates *et al*., 2000; da Costa Lima *et al*., 2010).

Aptamers are single-stranded oligonucleotide sequences that are DNA- or RNA-structured. It is usually isolated through a specific method known as "Systematic Evolution of Ligands by Exponential enrichment (SELEX)" (Sola *et al*., 2020; Al-Sudani *et al*., 2023; Patricia & Hailemeskel, 2024). By adopting stable, sequence-dependent three-dimensional conformations, these molecular recognition elements (Heo *et al*., 2016). Concerning leishmaniasis, aptamer-based molecular tools have been progressively developed against several Leishmanial-specific protein targets, including aptamer populations recognizing *L. infantum* kinetoplast membrane protein KMP-11 (Moreno *et al*., 2003), histone H2A (Ramos *et al*., 2007; Martín *et al*., 2013; Padma *et al*., 2023) and histone H3 (Ramos *et al*., 2010; Frezza *et al*., 2020), each showing nanomolar affinity and high specificity using ELONA, slot blot, and Western blot platforms (Brosseau *et al*., 2023; Bona *et al*., 2025).

Using SELEX against recombinant LiPABP, Guerra-Perez *et al*. (2015) (Prada *et al*., 2024) extended this pattern to PABP and isolated three high-affinity ssDNA aptamers: ApPABP#3, ApPABP#7, and ApPABP#11 (Kd = 5.4±1.1, 6.0±2.6, and 10.8±2.7 nM, respectively). Poly(A)-Sepharose competition assays revealed a crucial functional difference: ApPABP#11 specifically interrupted the LiPABP–poly(A) interaction, decreasing binding by about 30% for endogenous protein and 80% for recombinant LiPABP, whereas ApPABP#3 and ApPABP#7 showed no measurable impact on this interaction (Guerra-Pérez *et al*., 2015).

A crucial obstacle to aptamer-based intracellular pharmacological intervention is their intrinsic resistance to membrane penetration (Qusay *et al*., 2020). The negatively charged sugar-phosphate backbone of unmodified DNA prevents spontaneous cellular uptake, while extracellular nucleases degrade unprotected oligonucleotides within a few minutes (Balasegaram *et al*., 2012; Yoon & Rossi, 2018; Sakhnenkova *et al*., 2023). Both challenges can be simultaneously addressed by the liposomal reagents such as Lipofectamin®. Because of the high Transfection Efficiency (TE) for DNA, siRNA, and miRNA across several cell lines, especially those with poor transfection efficacy, Lipofectamine has been considered the "gold-standard" of transfection reagents, along with its ability to prolong the half-life of aptamers (Cao *et al*., 2009; Cardarelli *et al*., 2016; Saadati *et al*., 2024).

Despite these fundamental properties, the possible anti-leishmanial activity of PABP-targeting aptamers has not yet been thoroughly investigated in leishmania. No previous experimental study has examined whether molecular disruption of PABP activity by aptamers results in quantifiable growth suppression or alters protein expression in the parasite's clinically significant amastigote stage.

Therefore, the present study has investigated this point by evaluating the anti-leishmanial effects of lipofectamine-complexed ApPABP#7 and ApPABP#11 against *L. donovani* amastigotes.

Materials and Methods

This evaluation includes the use of MTT cytotoxicity assays to determine half-maximal inhibitory concentrations (IC_{50}) at 24 and 48 hours, and Western blot analysis to quantify PABP protein expression under two aptamer treatments (AP-7/LF and AP-11/LF) compared to untreated, lipofectamine-only, and free-aptamer controls.

Materials

aptamers oligonucleotides with a sequence of AP#7 (5'-CCAGAGTGAACACAAAGAAATTGAAATACGTAA GCTCCGG-3') and AP#11 (5'-GGCCCCCTCCTCCCTCCCCCACCCGACACTATTCCCCCC C-3') (Guerra-Pérez *et al*., 2015) were obtained from Macrogn®, South Korea. **Lipofectamine® 2000** was obtained from Invitrogen® Life Technologies, USA. **Sodium Stibogluconate** (SSG) (CAS NO. 16037-91-5) was obtained from Sigma Aldrich, Germany. ***L. donovani* isolate** (MHOM/IQ/2005/MRU15) was obtained by the Department of Biology/ College of Science/ University of Baghdad, which had been specifically characterized by PCR (Al-Halbosiy *et al*., 2020). **RAW 264.7 Cell Line** was obtained from the American Type Culture Collection (ATCC) (Nahi *et al*., 2025).

Aptamer Preparation

Lyophilized aptamers (AP#7 and AP#11) were first reconstituted to 100 µM stock solutions using nuclease-free water, then aliquoted and stored at -20°C for future use (Henri *et al*., 2019). On the day of the experiment, an aptamer working solution was prepared and folded to promote secondary/tertiary structure formation before application to the cells (Mayer & Menger, 2019; Tang *et al*., 2025).

Aptamer Transfection with Lipofectamine®2000

Aptamer was complexed with Lipofectamine®2000 (LF) according to the manufacturer's guidance for Lipofectamine®2000 complex formation. Briefly, three sterile tubes, Tube A (diluted Lipofectamine), Tube B (aptamer working solution), and Tube C (AP/LF complex) were prepared and labeled. The LF vial (1.5 ml kept at 4°C) was mixed gently and left for 5 minutes at room temperature (25°C) before use.

In Tube A, 1.5 µL LF was diluted in 125 µL Opti-MEM® (serum-free medium), mixed gently, and incubated 5 min at room temperature. In tube B, the aptamer working solution was prepared and folded as described above at double the desired final concentration. Then, in Tube C, equal volumes from Tube A and Tube B were combined, mixed gently, and incubated for 20 min at room temperature to allow the lipid–aptamer complex formation (Weissig, 2010; Technologies, 2000; Hussein *et al*., 2024).

Parasite Culture

L. donovani Promastigotes were cultured in RPMI-1640 medium (Capricorn Scientific®) supplemented with 10% heat inactivated fetal bovine serum (HIFBS) (Capricorn Scientific®), 100U/ml penicillin, and 100µg/ml streptomycin (Capricorn Scientific®), and incubated at 26°C. Amastigotes were differentiated in Modified Acidic Medium (MAA/20) by increasing the HIFBS to 20%, adjusting the pH to 5.5, and shifting the temperature to 37°C. Briefly, promastigotes at the stationary phase of growth, obtained after 8 days of incubation at 26°C and pH 7, were harvested and resuspended in prewarmed (37°C) modified MAA/20 medium. The amastigotes were obtained after 5 days of incubation. Cell counting was performed using the automated dual counting slide chambers (Bio-Rad, USA) (Clos, 2019)

Culturing of RAW 264.7 Cells

The RAW 264.7 cells were maintained in complete DMEM supplemented with 10% heat-inactivated fetal bovine serum (HI-FBS) and 1% penicillin/streptomycin (100 U/mL penicillin, 100 µg/mL streptomycin) at 37°C in a humidified incubator containing 5% CO_2.

RAW 264.7 Cells Infection with L. Donovani Parasites

When the culture of RAW 264.7 cells reached approximately 80% confluency, cells were harvested by trypsinization, re-suspended in complete DMEM, and counted using an automated cell counter. Then, cells are seeded at a concentration of 5×104/ well (2 ml) in a sterile 6-well plate previously supplemented with 2 mL of complete DMEM per well, incubated overnight at 37°C, 5% CO_2 to allow cell adherence and spread. Promastigotes of *L. donovani* were cultured in RPMI 1640, supplemented with 10% HIFBS and 1% penicillin-streptomycin at 26°C. Then, they were allowed to grow for 6 days until reaching the late stationary phase (metacyclic infective promastigotes).

On the day of infection, stationary-phase promastigotes were harvested by centrifugation at 1500g for 10 minutes at room temperature. To remove residual culture medium and dead parasites, the supernatant was discarded, and the parasite pellet was washed twice with sterile PBS. The washed pellet was then resuspended in pre-warmed (37°C) complete DMEM. Viable promastigotes are counted using an automated counter. Then the volume that needed to achieve a multiplicity of infection (MOI) of 10 parasites per macrophage cell (10/ 1) was calculated, which is equal to 5×10^5/ well.

Infection Procedure

The culture medium of the RAW 264.7 cells monolayer in the 6-well plate was replaced by 2mL of fresh, pre-warmed complete DMEM containing the calculated number of stationary phase promastigotes (5×10^5 parasites/well) in each well. Then, the plate was swirled gently to distribute the parasites evenly across the macrophage monolayer, and the plate was incubated at 37°C, 5% CO_2 for 6 hours to allow phagocytosis of promastigotes by the macrophages. After the infection period, the medium containing non-internalized (extracellular) promastigotes was carefully aspirated, followed by 3 gentle washes with 2 mL of pre-warmed sterile PBS; after the last wash, 2 mL of fresh complete DMEM (37°C) was added to each well. The plate was then incubated at 37°C, 5% CO_2 incubator for 24 hours to allow complete transformation of internalized promastigotes into the amastigote form within the phagolysosome compartment of the macrophages. Twenty four hours post-infection, the medium was discharged from the wells and replaced with fresh complete DMEM containing the aptamer/lipofectamine complexes (AP-7/LF and AP-11/LF) at the IC_{50} concentrations of 460 and 80nM, respectively, along with the control groups (untreated cells, lipofectamine-only, and free aptamer) and the plate was incubated at 37°C, 5% CO_2 for 48 hours post-treatment, then proceeded to total protein extraction and western blot assay.

MTT Assay

The antileishmanial activity of the AP-11/LF complex was assessed using a colorimetric 3-(4,5-dimethylthiazol-2-yl)-2,5-diphenyltetrazolium bromide MTT cell proliferation and cytotoxicity as-say kit (Elabscience®). Briefly, log-phase amastigotes were seeded into 96-well plates (Nest, USA) at 1×10^6 parasites/mL (100 µL per well) in RPMI-1640 supplemented with 10% fetal bovine serum (FBS). Five experimental conditions were evaluated: (i) AP-11/LF complexes prepared as two-fold serial dilutions (1600, 800, 400, 200, 100, 50, 25, and 12.5 nM); (ii) LF-free aptamer (FAP) comprising AP-11 alone (1600 nM); (iii) LF-only carrier control consisting of diluted Lipofectamine without aptamer; (iv) sodium stibogluconate (SSG) as the positive control; and (v) untreated para-site cultures as the negative control. The FAP and LF-only groups were included to verify that ob-served effects were specifically attributable to the formulated AP-11/LF complex. 20 µL of each of the first four groups was added to their corresponding wells. After 24 and 48 hours of incubation at 37°C, the plates were ready for the MTT assay. A 0.5 mg/ml of MTT reagent was applied to each well of the five groups and incubated for 4 hours at 37°C, then dimethyl sulfoxide (DMSO) was added at a concentration of 0.5 % v/v to dissolve the formazan crystals after the medium containing the MTT solution was disposed of. The plate was shaken for 5 minutes, and cell viability was analyzed by plotting absorbance against concentration using the microplate reader (Bio-Rad, USA) at 570nm (with a 630nm reference wavelength); IC_{50} was calculated after 24 and 48 hours by plotting growth inhibition against log concentration. The compounds and controls were examined in triplicate for every assay. Parasite viability was calculated according to the equation:

To assess the selectivity of the aptamer/LF complexes, the cytotoxic effect on uninfected host cells was evaluated using the same MTT assay procedure. Briefly, RAW 264.7 macrophages were seeded into 96-well plates at 1×10^4 cells/well in 100 µL of complete DMEM and incubated overnight at 37°C with 5% CO_2 to allow adherence. Cells were then treated with AP-7/LF and AP-11/LF complexes across extended two-fold serial dilution ranges (625–80000 nM for AP-7/LF and 100–12800 nM for AP-11/LF) to ensure that the half-maximal cytotoxic concentration (CC_{50}) could be reached. LF-free aptamer, LF-only, and untreated groups were included as controls. After 24 and 48 hours of incubation, the MTT reagent was applied, and the assay was developed identically to the antiparasitic procedure described above. Macrophage viability was calculated using the same equation, and the CC_{50} was

determined by nonlinear regression (4PL model) in GraphPad Prism 8.0.2. If viability remained above 50% at the highest tested concentration, CC_{50} was reported as greater than that concentration. The selectivity index (SI) was calculated for each aptamer at each time point according to the following equation (Nahi *et al*., 2025):

$$SI = \frac{CC_{50}\ (RAW\ 264.7)}{IC_{50}\ (L.\ donovani\ amastigotes)} \quad (1)$$

SI > 10 was considered indicative of acceptable selective toxicity toward the parasite over the host cell.

Total Protein Extraction

Total protein was extracted from axenic and intracellular amastigotes using a bicinchoninic acid (BCA) total protein assay kit (Elabscience Biotec., USA). Briefly, harvested amastigote parasites were washed three times with ice-cold 1×PBS and resuspended in freshly prepared RIPA lysis buffer (working solution). The resulting lysates were sonicated for 30 min in an ice-cooled water bath sonicator and subsequently clarified by centrifugation at 12,000g for 10 min at 4 °C. Protein concentration in the collected supernatants was quantified using the BCA assay by measuring absorbance at 562 nm, and concentrations calculated from a bovine serum albumin (BSA) standard curve.

For the extraction of the total protein from the amastigotes phagocytized inside the macrophage cells (intracellular amastigotes), additional steps were performed to ensure complete disruption of the additional walls surrounding the amastigote cells. Using a pre-chilled plastic cell scraper, the cell monolayer was thoroughly scraped from the surface of each well while keeping the plate on ice. The lysate was then transferred into a correspondingly labeled, pre-chilled 1.5 mL microcentrifuge tube and submerged completely in a dry ice/ethanol bath (approximately -80°C) for 2 minutes. The tubes were then removed and transferred to a 37°C water bath for about 2 minutes until the contents are fully thawed, and once fully thawed, it is vortexed vigorously for 15 seconds, then returned to the ice and this cycle repeated 2 times again, followed by 15 minutes sonication in an ice-cooled water bath sonicator and finally clarified by centrifugation at 12,000g for 10 min at 4 °C (Fernandez-Becerra *et al*., 2023).

Western Blot Analysis

Using a Western blot detection kit (Elabscience Biotec., USA), equal amounts of protein were combined with 5× SDS loading buffer and denatured at 95°C for 5 min using a dry heating block. Samples were loaded on 4-12% NZY Bis-Tris precast gels (12-well format; NZY Tech, Portugal) alongside a pre-stained protein ladder. Proteins were subsequently transferred to a 0.45 µm Poyvinylidene difluoride (PVDF) membrane and blocked with 5% (w/v) skimmed milk in Tris-buffered saline containing 0.1% Tween-20 (TBST) for 90 min at room temperature. Membranes were incubated overnight at 4° C on a rocker with the primary antibody against PABPC1 (Elabscience Bio-Tec., USA) diluted 1:1000 in 5% skimmed milk/TBST, followed by three washes with 1× TBST. The membranes were then incubated for 60 min with HRP-conjugated anti-rabbit IgG secondary antibody (Elabscience Biotec., USA) diluted in 2% skimmed milk/TBST. After three additional TBST washes, immunoreactive bands were detected using enhanced chemiluminescence (ECL substrates A and B mixed 1:1). Signal intensities were quantified by band densitometry using the imaging system Molecular Imager® ChemiDocTM XRS+ (Bio-Rad Laboratories, France). Relative PABP expression was calculated following normalization to GAPDH and expressed as fold-change relative to untreated controls. Band intensities were quantified using ImageJ® software (Talib *et al*., 2020; Fernandez-Becerra *et al*., 2023).

Statistical Analysis

GraphPad Prism® version 8.0.2 was used for data analysis. All data were represented as the mean±standard error of means (SEM). The percentage of growth inhibition was derived from triplicate viability values (n=3) at each concentration and time point. The value of half-maximal inhibitory concentration (IC_{50}) was determined by the "nonlinear regression analysis" of the dose-response curve, while one-way ANOVA with Tukey post hoc test was used for group comparisons (all pairwise comparisons). $P < 0.05$ was considered statistically significant.

Results and Discussion

Dose-Dependent Growth Inhibition of Amastigotes

AP-11/LF yielded IC_{50} values of 130 nM at 24 hours and 80 nM at 48 hours across the tested concentration range of 12.5-1600 nM **(Figures 1a and 1b)**.

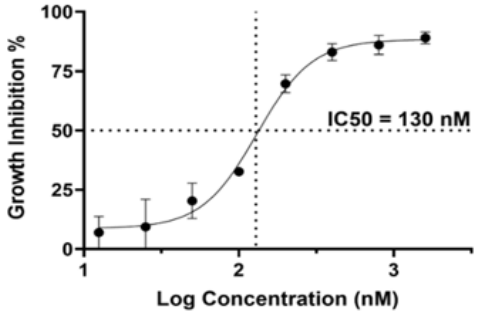

a)

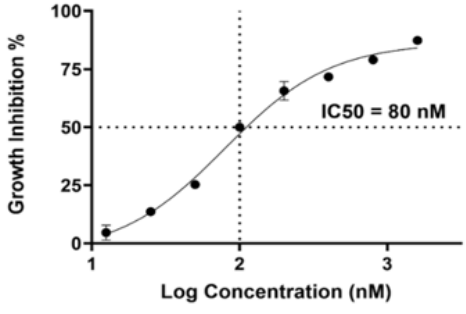

b)

Figure 1. Dose-response inhibition curve of *L. donovani* amastigotes by Aptamer-11 complexed with lipofectamine 2000 (AP11/LF). Growth inhibition % was calculated using

the MTT assay after being incubated with (12.5-1600 nM) doubling down dilution of AP-11/LF for 24 hours (a) and 48 hours (b). Nonlinear regression (4PL variable slope model) was used for Curves fitting. IC_{50} values were approximately 130nM (24 h) and 80nM (48 h). Data represent mean±SEM (n = 3).

In contrast, AP-7/LF required markedly higher concentrations to achieve growth suppression, with IC50 values of 550 nM at 24 hours and 460 nM at 48 hours across the range of 78.125-10000 nM **(Figures 2a and 2b)**.

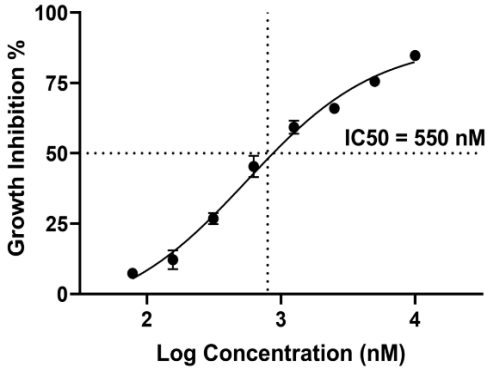

a)

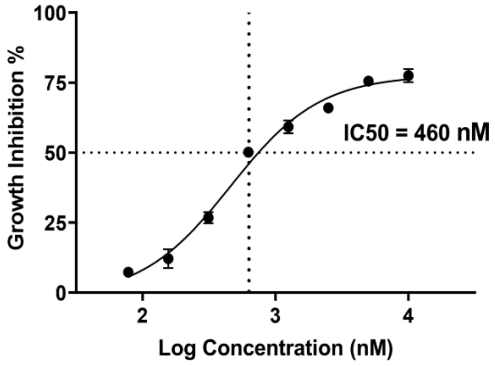

b)

Figure 2. Dose-response inhibition curves of *L. donovani* amastigotes treated with AP-7 complexed with Lipofectamine 2000 (AP-7/LF). Growth inhibition (%) was determined by MTT assay following incubation with two-fold serial dilutions of AP-7/LF (78.125–1000 nM) for 24 hours (a) and 48 hours (b). Curves were fitted by nonlinear regression (4PL variable slope model). IC_{50} values were approximately 550 nM (24 h) and 460 nM (48 h). Data represent mean±SEM (n = 3).

Host-Cell Cytotoxicity and Selectivity Indices

The CC50 values for AP-7/LF on macrophages were 40000 nM (40 µM) at 24 hours and 21500 nM (21.5 µM) at 48 hours **(Figures 3a and 3b)**, while those for AP-11/LF were 8330 nM (8.3 µM) at 24 hours and 6725 nM (3.8 µM) at 48 hours **(Figures 3c and 3d)**.

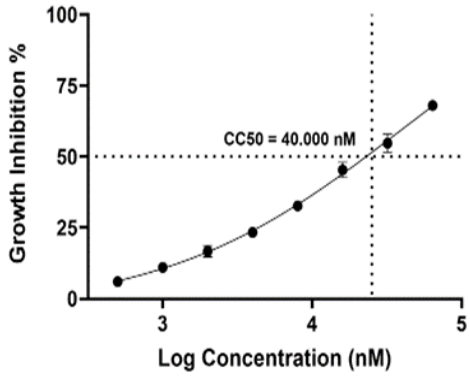

a)

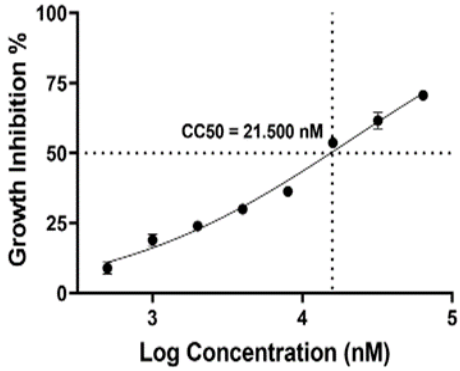

b)

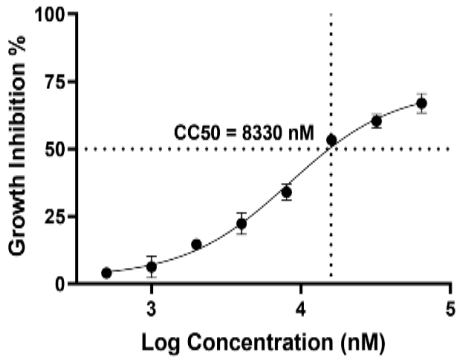

c)

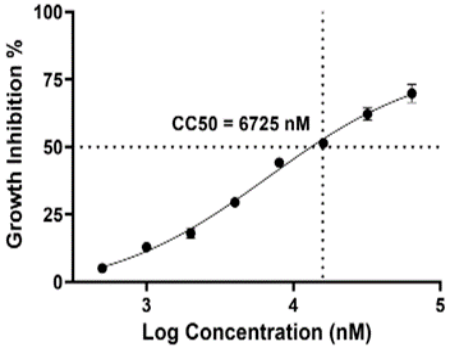

d)

Figure 3. Cytotoxicity of PABP-targeting aptamer/LF complexes on uninfected RAW 264.7 macrophages. Macrophage viability (%) was determined by MTT assay

following incubation with two-fold serial dilutions of AP-7/LF (625–80000 nM) for 24 hours (a) and 48 hours (b), and AP-11/LF (100–12800 nM) for 24 hours (c) and 48 hours (d). Curves were fitted by nonlinear regression (4PL variable slope model). CC_{50} values for AP-7/LF were approximately 40000 nM (24 h) and 21500 nM (48 h); CC_{50} values for AP-11/LF were approximately 8330 nM (24 h) and 6725 nM (48 h). Selectivity indices (SI = CC_{50}/IC_{50}): AP-7/LF, SI = 72.7 (24 h) and 46.7 (48 h); AP-11/LF, SI = 64 (24 h) and 84 (48 h); All SI values exceeded the accepted threshold of 10 for selective antiparasitic activity. Data represent mean±SEM (n = 3).

The selectivity indices (SI = CC50 [RAW 264.7] / IC_{50} [*L. donovani* amastigotes]) calculated for each aptamer at each time point were as follows: AP-7/LF, SI = 72.7 (24 h) and 46.7 (48 h); AP-11/LF, SI = 64 (24 h) and 84 (48 h).

PABP Expression in Amastigotes

In the AP-7/LF-treated amastigotes, PABP expression was reduced to approximately 0.55 compared to the control, representing a moderate reduction of approximately 45% **(Figures 4a and 4b)**. This reduction reached statistical significance compared with both the LF-only carrier ($p < 0.05$) and the free aptamer FAP-7 ($p < 0.05$), although the magnitude of the effect was substantially smaller than that observed with AP-11/LF. Neither the LF-only nor the FAP-7 group differed significantly from the untreated control.

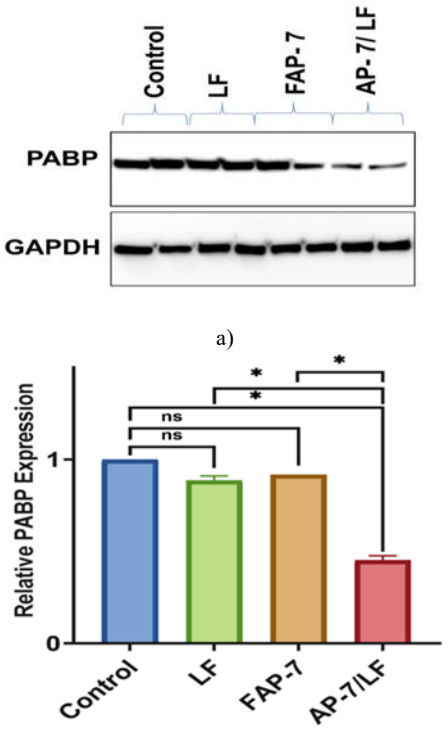

Figure 4. Effect of AP-7/LF on PABP protein expression in *L. donovani* amastigotes. (a) Representative western blot showing PABP and GAPDH expression in untreated control, LF-only, FAP-7, and AP-7/LF-treated group. (b) Densitometric quantification of PABP normalized to GAPDH and expressed compared to untreated control. AP-7/LF reduced PABP expression to approximately 0.55 (~45% reduction). Data represent mean±SEM of independent experiments. Statistical significance was determined by one-way ANOVA followed by Tukey post-hoc test. ns: not significant; *: $p < 0.05$.

In amastigotes treated with AP-11/LF, PABP band intensity was dramatically reduced to approximately 0.07 compared to the untreated control following GAPDH normalization **(Figure 5a and 5b)**.

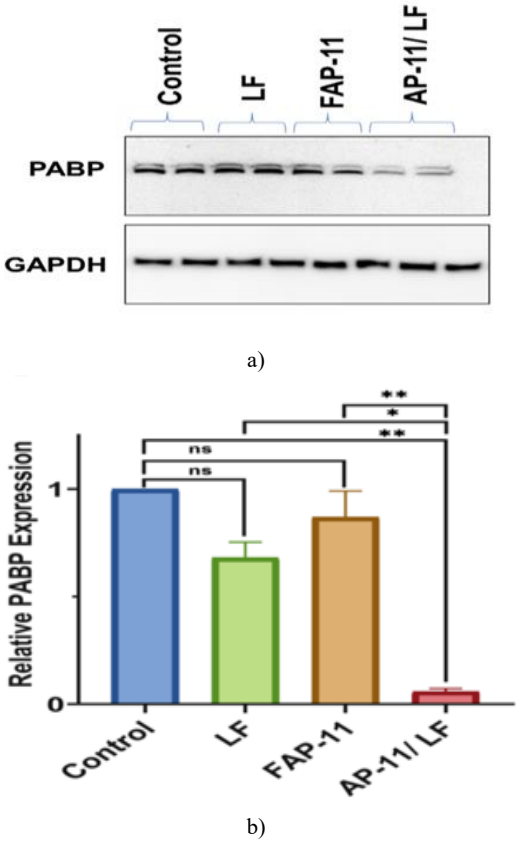

Figure 5. Effect of AP-11/LF on PABP protein expression in *L. donovani* amastigotes. (a) Representative western blot showing PABP and GAPDH (loading control) expression in untreated control parasites, Lipofectamine carrier alone (LF), LF-free aptamer-11 (FAP-11), and AP-11/LF-treated group. (b) Densitometric quantification of PABP band intensity normalized to GAPDH and expressed compared to untreated control (set to 1.0). AP-11/LF reduced PABP expression to approximately 0.07 (>93% reduction). Data represent mean±SEM of independent experiments. Statistical significance was determined by one-way ANOVA followed by Tukey post-hoc test. ns: not significant; *: $p < 0.05$; **: $p < 0.01$.

This reduction, corresponding to a greater than 93% depletion of detectable PABP protein, was highly significant when compared

with the untreated control ($p < 0.01$), the LF-only group ($p < 0.01$), and the LF-free aptamer group FAP-11 ($p < 0.01$). Neither the LF-only nor the FAP-11 control groups exhibited statistically significant changes in PABP expression compared to untreated parasites.

PABP Expression in Intracellular Amastigotes

For AP-7/LF in the intracellular setting, PABP expression was reduced to approximately 0.5 compared to control, a magnitude comparable to that observed in the axenic experiment **(Figures 6a and 6b)**. However, in contrast to the axenic results, this reduction did not reach statistical significance for any pairwise comparison. All comparisons between the AP-7/LF group and the control, LF-only, and FAP-7 groups were non-significant. AP-11/LF reduced PABP expression to approximately 0.2 compared to the untreated infected control **(Figures 7a and 7b)**, representing an approximately 80% reduction. This effect was statistically significant compared with the untreated control ($p < 0.01$), the LF-only group ($p < 0.05$), and the FAP-11 group ($p < 0.05$). As in the axenic model, neither the LF-only nor the FAP-11 control groups showed significant alterations in PABP expression.

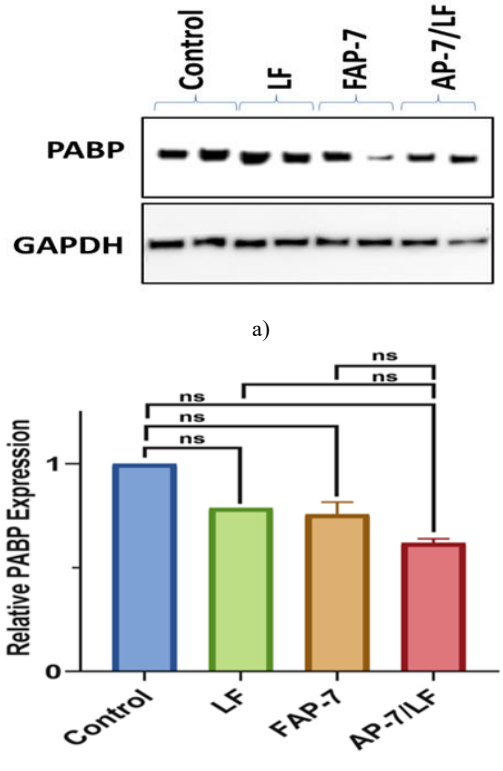

Figure 6. Effect of AP-7/LF on PABP protein expression in intracellular *L. donovani* amastigotes within RAW 264.7 macrophages. (a) Representative western blot showing PABP and GAPDH expression in untreated infected macrophages (Control), LF-only, FAP-7, and AP-7/LF-treated groups. Infected macrophages were treated at the 48-hour amastigote IC_{50} concentration. (b) Densitometric quantification of PABP normalized to GAPDH and expressed compared to untreated infected control. AP-7/LF reduced PABP expression to approximately 0.5 (~50% reduction); however, none of the pairwise comparisons reached statistical significance. Data represent mean±SEM of independent experiments. Statistical significance was determined by one-way ANOVA followed by Tukey post-hoc test. ns: not significant.

AP-11/LF reduced PABP expression to approximately 0.2 relative to the untreated infected control **(Figures 7a and 7b)**, representing an approximately 80% reduction. This effect was statistically significant compared with the untreated control ($p < 0.01$), the LF-only group ($p < 0.05$), and the FAP-11 group ($p < 0.05$). As in the axenic model, neither the LF-only nor the FAP-11 control groups showed significant alterations in PABP expression.

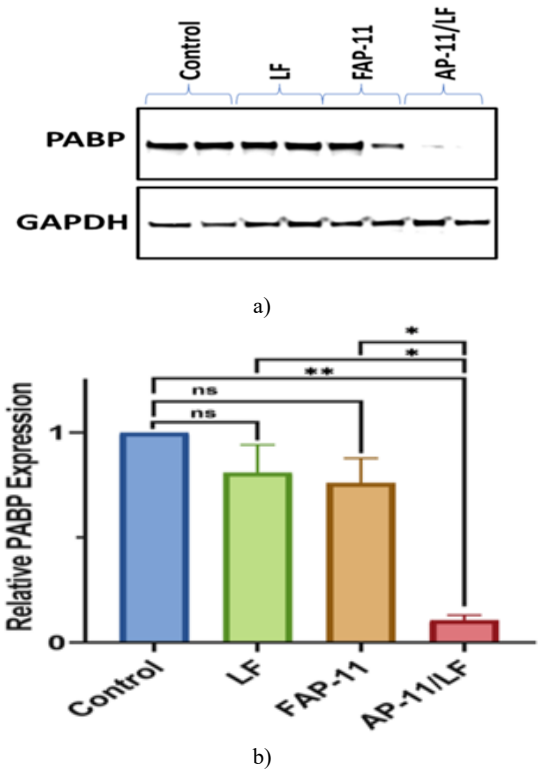

Figure 7. Effect of AP-11/LF on PABP protein expression in intracellular *L. donovani* amastigotes within RAW 264.7 macrophages. (a) Representative western blot showing PABP and GAPDH expression in untreated infected macrophages (Control), LF-only, FAP-11, and AP-11/LF-treated groups. Infected macrophages were treated at the 48-hour amastigote IC_{50} concentration. (b) Densitometric quantification of PABP normalized to GAPDH and expressed compared to untreated infected control. AP-11/LF reduced PABP expression to approximately 0.2 (~80% reduction). Data represent mean±SEM of independent experiments. Statistical significance was determined by one-way ANOVA followed by Tukey post-hoc test. ns: not significant; *: $p < 0.05$; **: $p < 0.01$.

Among the spectrum of challenges in people infected with visceral leishmaniasis, the treatment of the disease still constitutes a distinct obstacle, as it still has limited options due to resistance, toxicity,

and parenteral administration (Ponte-Sucre *et al*., 2017; Zurlo *et al*., 2025). Recent studies have called for alternative therapeutic means, especially those with novel molecular targets, including nucleic acid targeting modules (Sujith *et al*., 2024). Accordingly, the current study presents the first trial in this context as it evaluated two ssDNA aptamers targeting the PABP of *Leishmania donovani*, converting them to an attractive experimental validated antileishmanial therapy.

The cytotoxicity test disclosed a potency gap between the two aptamer complexes across all tested concentrations. In the infected macrophage cells, the AP-11/LF inhibited the growth of the amastigotes with an IC_{50} 4-times lower at 24 hours and around 6-times lower at 48 hours than that of AP-7/LF complex. Whereas in the cultured promastigote, the gap increased to about 8 times at 24 hours and 7 times at 48 hours, respectively. These disparities reflect the differences in affinity of the aptamers for protein PABP, as determined by Guerra-Perez *et al*. (2015); (Jegede, 2024). The fact that aptamers with low affinity stimulate a stronger biological effect suggests that the functional consequence of binding, specifically the disruption of interaction between the poly(A) and its binding protein (PABP), is the critical determining step of the antiparasitic activity, and not the binding strength alone. This is consistent with Guerra-Perez *et al*. (2015), where they claimed that Ap-11 was the only aptamer that decreased the poly(A) binding by 30% for the endogenous and 80% for the recombinant PABP, while AP-7 had no detectable effect on this interaction. Additionally, when comparing the range of IC_{50} nanomolar values of AP-11/LF with the recorded values of the traditional antileishmanial drugs, the observed values of the current study represent a favorable range of reported values. Miltefosine, for example, has been reported to inhibit *L. donovani* amastigotes with an IC_{50} of 0.4-3.8 μM. (Yoon & Rossi, 2018). Other recently identified synthetic flavonoid compounds 7, 11, and 14 against *L. donovani* produce IC_{50} values of 1.7 to 3.6 μM with selectivity indices of 29.9 for compound 14 (Callahan *et al*., 1997). Another antileishmanial compound, the enantiomer of lycorine, BMD-NP-00820, showed anti-amastigote activity with an IC_{50} value of 1.74±0.27 μM and a SI > 29. This result, thus, represents a noticeable potency for AP-11/LF against other reagents (Phan *et al*., 2024).

The results of the western blot also differentiate between two different modes of PABP modification. The semi-total depletion of the detectable protein produced by AP-11/LF (93% and 80% in and intracellular amastigotes, respectively) represents a degree of reduction that is incompatible with the simple steric blockade, as the PABP will remain physically intact and detectable at control levels (Bag & Bhattacharjee, 2010) . Displacement from poly(A) substrate could trigger an active degradation pathway. Regarding AP-7/LF, it reduced PABP expression by 45-50% without significant results in the intracellular model, which is consistent with the fact that binding at a topographically distant site from the poly(A) recognition domain (Guerra-Pérez *et al*., 2015) leads to a non-significant destabilization by allosteric disruption without significant triggering of protein loss associated with poly(A)-competitive antagonism.

On the other hand, AP-11/LF still has the activity of PABP depletion within the infected macrophages ($p < 0.01$ vs. control), demonstrating that Lipofectamine can penetrate the macrophage plasma membrane and the parasitophorous vacuole membrane to reach the intracellular targets at a functionally effective concentration (Al-Halbosiy *et al*., 2020). However, AP-7/LF was not statistically significant, which may be caused by the intrinsic variability of the intracellular system that complexed with the moderate biological effect, which aligns with the hypothesis that poly(A) competitive disruption represents the mechanistically decisive step. This differential response between the two aptamers supports the fact that PABP stability in Leishmania is directly related to the integrity of its poly(A) binding function (Vinet *et al*., 2009; Bag & Bhattacharjee, 2010). Regarding the role of the formulation controls FAP and LF, neither one of them has produced a significant reduction in any experimental model, indicating that the observed effects are strictly attributed to the intracellular delivered aptamers binding their target. Failure of the free aptamers to affect the protein confirms the delivery barriers and that aptamers cannot access their intracellular target without the Lipofectamine, regardless of their binding affinity (Chandola *et al*., 2016; Barreiro-Costa *et al*., 2022).

Conclusion

This study establishes, through direct comparative analysis, that the antiparasitic potency of PABP-targeting aptamers against *L. donovani* is directed principally by their capacity to disrupt the PABP-poly(A) interaction rather than by binding affinity alone. AP-11, the sole poly(A)-competitive antagonist, produced dose-dependent growth inhibition at nanomolar concentrations, near-complete PABP protein depletion in amastigotes, and statistically significant PABP reduction in the intracellular macrophage model, all with selectivity indices exceeding 84. AP-7, which binds a functionally silent PABP epitope with high affinity, produced weaker and less consistently significant effects across all endpoints. Together, these findings validate PABP as a pharmacologically tractable target in leishmania, specify the mechanistic requirements for effective PABP-directed therapy, and provide a rational foundation for the development of optimized aptamer-based antileishmanial agents.

Acknowledgments: The authors are grateful to the Mustansiriyah University and Ninevah University for their support to accomplish this study.

Conflict of interest: None

Financial support: None

Ethics statement: The study was approved by College of Pharmacy/Mustansiriyah University (Approval Letter Number 1413 on 03 April 2024).

References

Al Nasser, W. A., Al Ibrahim, H. M., Al Atieah, M. M., Al Ameen, R. A. A., Albeladi, M. S., Alshahrani, S. A., Alabdultiaf, S. H. A., Al Daihnayn, A. H., Al-Awami, H. A., Abuqurain, K.

A., et al. (2024). Visceral leishmaniasis: A comprehensive review. *Zenodo, 3*, 82–85. doi:10.5281/zenodo.14270442

Al-Halbosiy, M. M. F., Ali, H. Z., Hassan, G. M., & Ghaffarifar, F. (2020). Artemisinin efficacy against Old World Leishmania donovani: In vitro and ex vivo study. *Annals of Parasitology, 63*(3), 295–302. doi:10.17420/ap6603.267

Alqara, M. H., Alqara, A. H., & AlKhathlan, A. (2024). Recent advances in minimally invasive dentistry: A narrative review of the literature. *Annals of Dental Speciality, 12*(3), 28–33. doi:10.51847/GdquefIPmp

Al-Sudani, B. T., Mohammed, A. A., & Talib, L. J. (2023). Drug discovery and antiproliferative effect of linear and circular aptamers on colon cancer. *Journal of Pharmaceutical Negative Results, 14*(2), 1526–1535.

Assis, L. A., Santos Filho, M. V. C., da Cruz Silva, J. R., Bezerra, M. J. R., de Aquino, I. R. P. U. C., Merlo, K. C., Holetz, F. B., Probst, C. M., Rezende, A. M., Papadopoulou, B., et al. (2021). Identification of novel proteins and mRNAs differentially bound to the Leishmania poly(A) binding proteins reveals a direct association between PABP1, the RNA-binding protein RBP23, and mRNAs encoding ribosomal proteins. *PLOS Neglected Tropical Diseases, 15*(10), e0009899. doi:10.1371/journal.pntd.0009899

Bag, J., & Bhattacharjee, R. B. (2010). Multiple levels of post-transcriptional control of expression of the poly(A)-binding protein. *RNA Biology, 7*(1).

Balasegaram, M., Ritmeijer, K., Lima, M. A., Burza, S., Ortiz Genovese, G., Milani, B., Gaspani, S., Potet, J., & Chappuis, F. (2012). Liposomal amphotericin B as a treatment for human leishmaniasis. *Expert Opinion on Emerging Drugs, 17*(4), 493–510. doi:10.1517/14728214.2012.748036

Barreiro-Costa, O., Quiroga Lozano, C., Muñoz, E., Rojas-Silva, P., Medeiros, A., Comini, M. A., & Heredia-Moya, J. (2022). Evaluation of the anti-Leishmania mexicana and -Trypanosoma brucei activity and mode of action of 4,4'-(arylmethylene)bis(3-methyl-1-phenyl-1H-pyrazol-5-ol). *Biomedicines, 10*(8), 1913. doi:10.3390/biomedicines10081913

Bates, E. J., Knuepfer, E., & Smith, D. F. (2000). Poly(A)-binding protein I of Leishmania: Functional analysis and localization in trypanosomatid parasites. *Nucleic Acids Research, 28*(5), 1211–1220.

Berry, I., & Berrang-Ford, L. (2016). Leishmaniasis, conflict, and political terror: A spatio-temporal analysis. *Social Science & Medicine, 167*, 140–149. doi:10.1016/j.socscimed.2016.04.038

Berzal-Herranz, A., & Romero-López, C. (2024). Aptamers' potential to fill therapeutic and diagnostic gaps. *Pharmaceuticals (Basel, Switzerland), 17*(1), 105. doi:10.3390/ph17010105

Bona, C., Camacho-Alonso, F., Vaca, A., & Llorente-Alonso, M. (2025). Oral biofilm control in patients using orthodontic aligners: Evidence from a systematic review. *Asian Journal of Periodontics and Orthodontics, 5*, 33–42. doi:10.51847/siIhUaqfip

Brosseau, N. E., Vallée, I., Mayer-Scholl, A., Ndao, M., & Karadjian, G. (2023). Aptamer-based technologies for parasite detection. *Sensors, 23*(2), 562. doi:10.3390/s23020562

Callahan, H. L., Portal, A. C., Devereaux, R., & Grogl, M. (1997). An axenic amastigote system for drug screening. *Antimicrobial Agents and Chemotherapy, 41*(4), 818–822. doi:10.1128/AAC.41.4.818

Cao, Z., Tong, R., Mishra, A., Xu, W., Wong, G. C., Cheng, J., & Lu, Y. (2009). Reversible cell-specific drug delivery with aptamer-functionalized liposomes. *Angewandte Chemie International Edition, 48*(35), 6494–6498. doi:10.1002/anie.200901452

Cardarelli, F., Digiacomo, L., Marchini, C., Amici, A., Salomone, F., Fiume, G., Rossetta, A., Gratton, E., Pozzi, D., & Caracciolo, G. (2016). The intracellular trafficking mechanism of Lipofectamine-based transfection reagents and its implication for gene delivery. *Scientific Reports, 6*, 25879. doi:10.1038/srep25879

Chandola, C., Kalme, S., Casteleijn, M. G., Urtti, A., & Neerathilingam, M. (2016). Application of aptamers in diagnostics, drug-delivery and imaging. *Journal of Biosciences, 41*(3), 535–561. doi:10.1007/s12038-016-9632-y

Clos, J. (Ed.). (2019). *Leishmania: Methods and Protocols*. Springer Nature. doi:10.1007/978-1-4939-9210-2

da Costa Lima, T. D., Moura, D. M., Reis, C. R., Vasconcelos, J. R., Ellis, L., Carrington, M., Figueiredo, R. C., & de Melo Neto, O. P. (2010). Functional characterization of three Leishmania poly(A) binding protein homologues with distinct binding properties to RNA and protein partners. *Eukaryotic Cell, 9*(10), 1484–1494. doi:10.1128/EC.00148-10

De Gaudenzi, J. G., Noé, G., Campo, V. A., Frasch, A. C., & Cassola, A. (2011). Gene expression regulation in trypanosomatids. *Essays in Biochemistry, 51*(1), 31–46. doi:10.1042/BSE0510031

Elango, R., & Govindaraju, L. (2025). In vitro evaluation of Kedo SDF gel effect on the micro-hardness of natural carious dentin. *Annals of Dental Speciality, 13*(2), 12–14. doi:10.51847/fQknFGnize

Fernandez-Becerra, C., Xander, P., Alfandari, D., Dong, G., Aparici-Herraiz, I., Rosenhek-Goldian, I., Shokouhy, M., Gualdron-Lopez, M., Lozano, N., Cortes-Serra, N., et al. (2023). Guidelines for the purification and characterization of extracellular vesicles of parasites. *Journal of Extracellular Biology, 2*(10), e117. doi:10.1002/jex2.117

Frezza, V., Pinto-Díez, C., Fernández, G., Soto, M., Martín, M. E., García-Sacristán, A., & González, V. M. (2020). DNA aptamers targeting Leishmania infantum H3 protein as potential diagnostic tools. *Analytica Chimica Acta, 1107*, 155–163. doi:10.1016/j.aca.2020.02.012

Guerra, N., Vega-Sendino, M., Pérez-Morgado, M. I., Ramos, E., Soto, M., Gonzalez, V. M., & Martín, M. E. (2011). Identification and functional characterization of a poly(A)-binding protein from Leishmania infantum (LiPABP). *FEBS Letters, 585*(1), 193–198. doi:10.1016/j.febslet.2010.11.042

Guerra-Pérez, N., Ramos, E., García-Hernández, M., Pinto, C., Soto, M., Martín, M. E., & González, V. M. (2015). Molecular and functional characterization of ssDNA

aptamers that specifically bind Leishmania infantum PABP. *PLOS ONE, 10*(10), e0140048. doi:10.1371/journal.pone.0140048

Hamad, M., Jaafar, N., Ahmed, O. H., & Abd, M. (2018). GC/MS analysis of terpenes of Boswellia serrata resin found in Iraq. *Journal of Global Pharma Technology, 10*, 290–294.

Henri, J., Bayat, N., Macdonald, J., & Shigdar, S. (2019). A guide to using nucleic acid aptamers in cell-based assays.

Heo, K., Min, S. W., Sung, H. J., Kim, H. G., Kim, H. J., Kim, Y. H., Choi, B. K., Han, S., Chung, S., Lee, E. S., et al. (2016). An aptamer-antibody complex (oligobody) as a novel delivery platform for targeted cancer therapies. *Journal of Controlled Release, 229*, 1–9. doi:10.1016/j.jconrel.2016.03.006

Huata-Panca, P., Apaza, J. M. H., Carita, A. J. Q., Mamani, G. Q., & Torres-Cruz, F. (2025). Determinants of mortality type in a high altitude Andean context using a multivariable logit regression model in Puno, Peru. *Journal of Advanced Pharmacy Education and Research, 15*(3), 198–204. doi:10.51847/1vvhNPv5Vy

Hussein, N. R., Sahib, H. B., & Omran, Z. S. (2024). Anti-proliferative of phenyl isoserine derivative containing a 1,2,3-triazole ring on breast cancer cell line. *Journal of Advanced Pharmacy Education and Research, 14*(2), 110–119. doi:10.51847/xHUGpvrkc9

Jamal Talib, L., Talib Al-Sudani, B., & Ghazi Al-Abbassi, M. (2020). Aptamer validation by Western blot: An overview. *Al Mustansiriyah Journal of Pharmaceutical Sciences, 20*(4), 122-131.

Jegede, A. O. (2024). Comparison of job satisfaction among pharmacists in different practice settings in Nigeria. *Journal of Organizational Behavior Research, 9*(2), 28–41. doi:10.51847/Hx3ZrNIk4Z

Knight, C. A., Harris, D. R., Alshammari, S. O., Gugssa, A., Young, T., & Lee, C. M. (2023). Leishmaniasis: Recent epidemiological studies in the Middle East. *Frontiers in Microbiology, 13*, 1052478. doi:10.3389/fmicb.2022.1052478

Kumar, P., Kumar, P., Singh, N., Khajuria, S., Patel, R., Rajana, V. K., Mandal, D., & Velayutham, R. (2022). Limitations of current chemotherapy and future of nanoformulation-based AmB delivery for visceral leishmaniasis: An updated review. *Frontiers in Bioengineering and Biotechnology, 10*, 1016925. doi:10.3389/fbioe.2022.1016925

Life Technologies. (2000). *Lipofectamine® 2000 reagent protocol outline*. www.lifetechnologies.com/support

Martín, M. E., García-Hernández, M., García-Recio, E. M., Gómez-Chacón, G. F., Sánchez-López, M., & González, V. M. (2013). DNA aptamers selectively target Leishmania infantum H2A protein. *PLOS ONE, 8*(10), e78886. doi:10.1371/journal.pone.0078886

Martínez-Calvillo, S., Vizuet-de-Rueda, J. C., Florencio-Martínez, L. E., Manning-Cela, R. G., & Figueroa-Angulo, E. E. (2010). Gene expression in trypanosomatid parasites. *Journal of Biomedicine and Biotechnology, 2010*, 525241. doi:10.1155/2010/525241

Mayer, G., & Menger, M. M. (Eds.). (2019). *Nucleic Acid Aptamers: Selection, Characterization, and Application*. Springer. http://www.springer.com/series/7651

Moreno, M., Rincón, E., Piñeiro, D., Fernández, G., Domingo, A., Jiménez-Ruíz, A., Salinas, M., & González, V. M. (2003). Selection of aptamers against KMP-11 using colloidal gold during the SELEX process. *Biochemical and Biophysical Research Communications, 308*(2), 214–218. doi:10.1016/s0006-291x(03)01352-4

Nahi, S. A. A., Arif, I. S., Mohammed, A. A., & Talib, W. H. (2025). Potential anti-inflammatory impact of SIRT1 activator on RAW 264.7 cells: In vitro study. *Al Mustansiriyah Journal of Pharmaceutical Sciences, 25*(3), 445–454. doi:10.32947/ajps.v25i3.1215

Pacheco-Fernandez, T., Markle, H., Verma, C., Huston, R., Gannavaram, S., Nakhasi, H. L., & Satoskar, A. R. (2023). Field-deployable treatments for leishmaniasis: Intrinsic challenges, recent developments and next steps. *Research and Reports in Tropical Medicine, 14*, 61–85. doi:10.2147/RRTM.S392606

Padma, K. R., Don, K. R., Anjum, M. R., Sindhu, G. S., & Sankari, M. (2023). Application of green energy technology for environmental sustainability. *World Journal of Environmental Biosciences, 12*(4), 1–7. doi:10.51847/bAMKAPPZGe

Patricia, A., & Hailemeskel, B. (2024). Turmeric, black pepper, and lemon hot infusion for joint and musculoskeletal pain: A case report. *World Journal of Environmental Biosciences, 13*(1), 36–38. doi:10.51847/XeYTN4wNsa

Pham, T. T. (2024). Linking family supports and Vietnamese employee performance: The mediator role of work engagement. *Journal of Organizational Behavior Research, 9*(1), 15–31. doi:10.51847/W3DMjBBfqq

Phan, T. N., Lee, H., Baek, K. H., & No, J. H. (2024). Identification of novel flavonoids and ansa-macrolides with activities against Leishmania donovani through natural product library screening. *Pathogens (Basel, Switzerland), 13*(3), 213. doi:10.3390/pathogens13030213

Pokharel, P., Ghimire, R., & Lamichhane, P. (2021). Efficacy and safety of paromomycin for visceral leishmaniasis: A systematic review. *Journal of Tropical Medicine, 2021,* 8629039. doi:10.1155/2021/8629039

Ponte-Sucre, A., Gamarro, F., Dujardin, J. C., Barrett, M. P., López-Vélez, R., García-Hernández, R., Pountain, A. W., Mwenechanya, R., & Papadopoulou, B. (2017). Drug resistance and treatment failure in leishmaniasis: A 21st century challenge. *PLOS Neglected Tropical Diseases, 11*(12), e0006052. doi:10.1371/journal.pntd.0006052

Prada, A. M., Cicalău, G. I. P., & Ciavoi, G. (2024). Resin infiltration for white-spot lesion management after orthodontic treatment. *Asian Journal of Periodontics and Orthodontics, 4*, 19–23. doi:10.51847/ZTuGEanCSV

Qusay, A., Marie, N. K., & Al-Sudani, B. T. (2020). Utilization of natural stabilizer to prepare a liposomal conjugate for the newly developed aptamer. *Systematic Reviews in Pharmacy, 11*(7), 32–50. doi:10.31838/srp.2020.7.07

Ramos, E., Moreno, M., Martín, M. E., Soto, M., & González, V. M. (2010). In vitro selection of Leishmania infantum H3-binding ssDNA aptamers. *Oligonucleotides, 20*(4), 207–213. doi:10.1089/oli.2010.0240

Ramos, E., Piñeiro, D., Soto, M., Abanades, D. R., Martín, M. E., Salinas, M., & González, V. M. (2007). A DNA aptamer population specifically detects Leishmania infantum H2A antigen. *Laboratory Investigation, 87*(5), 409–416. doi:10.1038/labinvest.3700535

Saadati, N., Masihi, S., Abouali, N., Akiash, N., Jafari, R. M., & Tahmasebi, Y. (2024). Evaluation of the cardiac function using GLS in speckle tracking echocardiography in preeclampsia and IUGR patients. *Journal of Advanced Pharmacy Education and Research, 14*(4), 1–6. doi:10.51847/QvxatTLHKC

Sakhnenkova, T. I., Abdul-Kadyrova, L. R., Akhilgova, Z. A., Brovikova, A. A., Markov, O. O., Saribekyan, A. A., Sampiev, R. M., & Loginov, A. A. (2023). Morphological and biochemical analysis of 3D scaffold based on biocompatible polymer for tissue engineering. *Journal of Advanced Pharmacy Education and Research, 13*(3), 29–33. doi:10.51847/v8o0GbXJdN

Sola, M., Menon, A. P., Moreno, B., Meraviglia-Crivelli, D., Soldevilla, M. M., Cartón-García, F., & Pastor, F. (2020). Aptamers against live targets: Is in vivo SELEX finally coming to the edge? *Molecular Therapy – Nucleic Acids, 21*, 192–204. doi:10.1016/j.omtn.2020.05.025

Sujith, S., Naresh, R., Srivisanth, B. U., Sajeevan, A., Rajaramon, S., David, H., & Solomon, A. P. (2024). Aptamers: Precision tools for diagnosing and treating infectious diseases. *Frontiers in Cellular and Infection Microbiology, 14*, 1402932. doi:10.3389/fcimb.2024.1402932

Tang, Q., Mears, A., & Bonnaire, K. (2025). Injectable composite resin in orthodontics: A novel approach for optimized smile aesthetics. *Asian Journal of Periodontics and Orthodontics, 5*, 141–149. doi:10.51847/BM7GGShiQP

Thuy, V. T. T., Hung, D. N., Oanh, L. T. T., Tuyet, V. T. A., & Thu, B. T. (2023). Factors impact on business performance of enterprises: The case of Vietnam. *Journal of Organizational Behavior Research, 8*(2), 27–39. doi:10.51847/2itmiM3CoE

Uliana, S. R. B., Trinconi, C. T., & Coelho, A. C. (2018). Chemotherapy of leishmaniasis: Present challenges. *Parasitology*, *145*(4), 464–480. doi:10.1017/S0031182016002523

Vinet, A. F., Fukuda, M., Turco, S. J., & Descoteaux, A. (2009). The Leishmania donovani lipophosphoglycan excludes the vesicular proton-ATPase from phagosomes by impairing the recruitment of synaptotagmin V. *PLOS Pathogens, 5*(10), e1000628. doi:10.1371/journal.ppat.1000628

Wamai, R. G., Kahn, J., McGloin, J., & Ziaggi, G. (2020). Visceral leishmaniasis: A global overview. *Journal of Global Health Science, 2*(1). doi:10.35500/jghs.2020.2.e3

Weissig, V. (Ed.). (2010). *Liposomes: Methods and Protocols, Volume 1: Pharmaceutical Nanocarriers*. Springer Nature. doi:10.1007/978-1-60327-360-2

Yoon, S., & Rossi, J. J. (2018). Aptamers: Uptake mechanisms and intracellular applications. *Advanced Drug Delivery Reviews, 134*, 22–35. doi:10.1016/j.addr.2018.07.003

Zhang, S. X., Yang, G. B., Sun, J. Y., Li, Y. J., Yang, J., Wang, J. C., & Deng, Y. (2025). Global, regional, and national burden of visceral leishmaniasis, 1990–2021: Findings from the Global Burden of Disease Study 2021. *Parasites & Vectors, 18*(1), 157. doi:10.1186/s13071-025-06796-x

Zinoviev, A., & Shapira, M. (2012). Evolutionary conservation and diversification of the translation initiation apparatus in trypanosomatids. *Comparative and Functional Genomics, 2012*, 813718. doi:10.1155/2012/813718

Zurlo, M., Korres, D., & Machera, K. (2025). Development of descriptive mathematical models for different domains of gingival recession using multiple linear regression analysis. *Annals of Dental Speciality, 13*(1), 55–65. doi:10.51847/nK5JGp2gcz